Synthesis, Characterization, and Luminescence of β-Cyclodextrin Inclusion Compounds Containing Europium(III) and Gadolinium(III) Tris(β-diketonates)

Susana S. Braga,[†] Rute A. Sá Ferreira,[‡] Isabel S. Gonçalves,*[,†] Martyn Pillinger,[†] João Rocha,[†] José J. C. Teixeira-Dias,[†] and Luís D. Carlos*[,‡]

Department of Chemistry and Department of Physics, University of Aveiro, Campus de Santiago, 3810-193 Aveiro, Portugal

Received: February 11, 2002; In Final Form: May 15, 2002

β-Cyclodextrin (β-CD) inclusion compounds containing the lanthanide complexes $Eu(NTA)_3 \cdot xH_2O$ and $Gd(NTA)_3 \cdot xH_2O$ [NTA = 1-(2-naphthoyl)-3,3,3-trifluoroacetone)] were prepared by treating a saturated aqueous solution of β-CD with a solution of the complex in ethanol. The molar ratio of host to guest in the reaction was either 3:1 or 1:1, leading to products designated as $M(NTA)_3 \cdot 3\beta$-CD and $M(NTA)_3 \cdot \beta$-CD (M = Eu, Gd), respectively. The products were characterized in the solid state by elemental analysis, powder X-ray diffraction, thermogravimetric analysis, FTIR, and ^{13}C CP MAS NMR spectroscopy, indicating the formation of true inclusion compounds in which the naphthoyl moieties of the guest species are encapsulated within the β-CD cavities. The photoluminescence results, in particular the determination of the experimental intensity parameters Ω_2 and Ω_4, show that this encapsulation seems to modify essentially the second Eu^{3+} coordination shell, namely, the energy and the lifetime of the lowest triplet state of the naphthalene groups. The encapsulation induces emission from the singlet excited state of the ligands with the corresponding presence of an inefficient ligand-to-metal ion energy transfer step.

Introduction

Cyclodextrins (CDs) are an important class of molecular receptors in the field of supramolecular chemistry.[1] These cyclic oligosaccharides form inclusion complexes with smaller molecules that fit into their 5−8 Å cavity (6.0−6.5 Å in the case of β-CD[2]). If the guest molecule is a metallo-organic species, the cyclodextrin host can be considered as a second-sphere ligand noncovalently bonded to the first sphere ligand(s).[3] These types of inclusion complexes are of fundamental significance because the weaker categories of noncovalent bonding, e.g., van der Waals and charge transfer interactions, assume considerable importance. Particularly suitable guests are those bearing hydrophobic ligands such as cyclopentadienyl and η^6-arene groups. One of the main objectives of carrying out this chemistry is to modify the properties of the guest compared to the bulk material, e.g., in their nonlinear optical properties,[4] and ligand substitution/insertion reactions.[5] Recently, the inclusion compound of β-CD and tris(dibenzoylmethane)europium(III) dihydrate was reported.[6] It was found that the photoluminescent properties of the guest were significantly altered compared to those of the pure compound. In this paper we describe the synthesis and characterization of β-cyclodextrin inclusion compounds containing europium(III) and gadolinium(III) tris-[1-(2-naphthoyl)-3,3,3-trifluoroacetonate] complexes. The luminescence of rare earth or lanthanide tris-β-diketonates has been widely investigated because of the strong line emission important for luminescent and laser materials.[7,8] In particular, the luminescence features and the absolute quantum yields of europium(III) tris[1-(2-naphthoyl)-3,3,3-trifluoroacetonate] complexes, $Eu(NTA)_3 \cdot 2L$ (L = H_2O and DMSO, dimethyl sulfoxide), were recently reported.[9] The experimental quantum yield measured for $Eu(NTA)_3 \cdot 2DMSO$, 0.75, is one of the highest so far reported for solid-state europium complexes.[9] The aim of the present work is to see how inclusion complexation of the title complexes with β-cyclodextrin affects their photophysical properties.

Experimental Section

We present here the general methods and instrumentation. β-CD was obtained from Wacker Chemie (München) and recrystallized before use. 1-(2-naphthoyl)-3,3,3-trifluoroacetone was purchased from Aldrich and used as received. Infrared spectra were recorded on a Unican Mattson Mod 7000 FTIR spectrophotometer using KBr pellets. Thermogravimetric analysis (TGA) studies were performed using a Mettler TA3000 system at a heating rate of 5 K/min under a static atmosphere of air. Powder X-ray diffraction (XRD) data were collected on a Philips X'pert diffractometer using Cu-K_α radiation filtered by Ni (λ = 1.5418 Å). Microanalyses were performed at the Technical University of Munich. ^1H NMR spectra were measured in solution using a Bruker CXP 300 spectrometer. Room-temperature solid-state ^{13}C NMR spectra were recorded at 100.62 MHz on a (9.4 T) Bruker MSL 400P spectrometer. ^{13}C CP MAS NMR spectra were recorded with a 4.5 μs ^1H 90° pulse, 2 ms contact time, a spinning rate of 9 kHz, and 12 s recycle delays. Chemical shifts are quoted in parts per million from TMS. The photoluminescence spectra (14−300 K) were recorded on a Jobin Yvon-Spex spectrometer (HR 460) coupled to a R928 Hamamatsu photomultiplier. A 300 W Xe arc lamp coupled and a monochromator Jobin Yvon-Spex (TRIAX 180) was used as the excitation source. All the spectra were corrected for the response of the detector. The time-resolved measurements were carried out using a pulsed Xe arc lamp (5 mJ/pulse, 3μs

* Corresponding authors. FAX: +(351)-234-370084. E-mail: igoncalves@dq.ua.pt, and lcarlos@fis.ua.pt.
[†] Department of Chemistry.
[‡] Department of Physics.

10.1021/jp0204004 CCC: $22.00
Published on Web 10/16/2002

bandwidth) coupled to the monochromator Kratos GM-252 and a Spex 1934 C phosphorimeter.

Lanthanide Complexes

Eu(NTA)$_3$·2H$_2$O (1). Prepared as described in the literature.[10] Selected ν_{max}/cm^{-1} 3445s, 3061m, 2926m, 1611vs, 1592s, 1568m, 1532m, 1509m, 1459m, 1430m, 1385m, 1354m, 1295vs, 1251m, 1198s, 1164s, 1143s, 1070m, 960m, 863m, 793s, 748m, 685m, 571m (KBr). δ_H (300 MHz, ethanol-d_6, SiMe$_4$) 8.73 (s, br, naphth), 8.63−8.58 (m, naphth), 8.13−7.79 (m, naphth), 7.70−7.18 (m, naphth), 5.37 (s, CH). δ_C NMR (75.47 MHz, ethanol-d_6, SiMe$_4$) 132.13, 131.80, 126.85, 126.04, 125.60, 125.35, 125.10, 124.32, 123.98, 123.81, 123.15, 122.31, 122.09, 120.88, 120.63, 119.16, 119.05, 118.25 (all naphth-C), 116.96 (CF$_3$), 96.53, 95.08 (CH). ^{13}C CP MAS NMR: δ = 182.8 (br, CO), 128.3 (br, naphth-C), 91.6 (CH).

Ga(NTA)$_3$·2H$_2$O (2). Prepared as described in the literature.[10] Selected ν_{max}/cm^{-1} 3441s, 3057m, 2929m, 1614vs, 1594s, 1569m, 1535m, 1508m, 1457m, 1429m, 1367m, 1354m, 1296vs, 1252m, 1199s, 1137s, 1074m, 957m, 864m, 794s, 748m, 721m, 684s, 577m, 471m (KBr).

Synthesis of Inclusion Compounds

Reactions were carried out with molar ratios β-CD:M(NTA)$_3$ = 3 or 1, giving products designated as M(NTA)$_3$·3β-CD and M(NTA)$_3$·β-CD. In general, a solution of M(NTA)$_3$·2H$_2$O (0.076 mmol) in ethanol (7 mL) was added dropwise to a solution of β-CD (0.3 g, 0.23 mmol or 0.1 g, 0.076 mmol) in water (15 or 5 mL), and the mixture was kept at 40 °C for 24 h. The mixture was centrifuged, the supernatant was decanted, and the yellow powder was washed with water and dried in air at room temperature.

Eu(NTA)$_3$·3β-CD (3). Yield: 0.33 g, 91%. Anal. Calcd. for (EuC$_{42}$H$_{24}$F$_9$O$_6$)·(C$_{42}$H$_{70}$O$_{35}$)$_3$·27H$_2$O (4839.0): C, 41.70; H, 6.00; Eu, 3.14. Found: C, 41.91; H, 5.80; Eu, 2.90. Selected ν_{max}/cm^{-1} 3342vs, 2924m, 2893sh, 1671vs, 1640sh, 1625s, 1612sh, 1570m, 1534m, 1509m, 1456m, 1430m, 1414sh, 1383m, 1370m, 1333m, 1301s, 1251m, 1158s, 1125m, 1102m, 1080vs, 1055vs, 1027vs, 1002m, 946m, 937m, 862m, 796m, 754m, 703m, 685m, 650w, 607m, 574m, 529m, 474m, 446m, 402m (KBr). ^{13}C CP MAS NMR: δ = 136.4, 134.1, 132.9, 127.5, 124.7 (all naphth-C), 103.7 (br, β-CD, C-1), 92.8 (s, CH), 81.4 (β-CD, C-4), 72.9 (br, β-CD, C-2,3,5), 60.7 (β-CD, C-6).

Gd(NTA)$_3$·3β-CD (4). Yield: 0.31 g, 83%. Anal. Calcd. for (GdC$_{42}$H$_{24}$F$_9$O$_6$)·(C$_{42}$H$_{70}$O$_{35}$)$_3$·30H$_2$O (4898.3): C, 41.19; H, 6.05; Gd, 3.21. Found: C, 41.80; H, 5.87; Gd, 3.70. Selected ν_{max}/cm^{-1} 2925m, 1675vs, 1615vs, 1595s, 1570m, 1532m, 1506m, 1457m, 1429m, 1385m, 1368m, 1355m, 1334m, 1299m, 1251m, 1201m, 1157s, 1103m, 1080vs, 1056sh, 1030vs, 1002s, 962w, 947m, 937m, 863m, 793m, 752m, 705m, 685m, 609m, 577m, 526m, 473m (KBr).

Eu(NTA)$_3$·β-CD (5). Yield: 0.16 g, 91%. Anal. Calcd. for (EuC$_{42}$H$_{24}$F$_9$O$_6$)·(C$_{42}$H$_{70}$O$_{35}$)·13H$_2$O (2316.8): C, 43.55; H, 5.22; Eu, 6.56. Found: C, 43.58; H, 5.12; Eu, 6.50. Selected ν_{max}/cm^{-1} 3374vs, 3061sh, 2927m, 2898sh, 1638sh, 1620s, 1611vs, 1593s, 1570m, 1533m, 1509m, 1461m, 1431m, 1385m, 1355m, 1299vs, 1252m, 1199s, 1138s, 1078s, 1053sh, 1027vs, 1003sh, 959m, 937m, 863m, 825w, 796s, 758m, 721w, 704w, 684s, 572s, 520m, 472m (KBr). ^{13}C CP MAS NMR: δ = 134.0 (sh), 128.6 (br) (all naphth-C), 103.7 (br, β-CD, C-1), 93.0 (s, CH), 81.2 (β-CD, C-4), 72.8 (br, β-CD, C-2,3,5), 60.1 (β-CD, C-6).

Gd(NTA)$_3$·β-CD (6). Yield: 0.09 g. Anal. Calcd. for (GdC$_{42}$H$_{24}$F$_9$O$_6$)·(C$_{42}$H$_{70}$O$_{35}$)·15H$_2$O (2358.1): C, 42.78; H, 5.30; Gd, 6.67. Found: C, 41.10; H, 4.90; Gd, 4.20. Selected ν_{max}/cm^{-1} 3374vs, 2926m, 2858sh, 1676vs, 1615s, 1597sh, 1532m, 1509m, 1459m, 1432m, 1384w, 1368m, 1354w, 1299vs, 1253m, 1201m, 1156s, 1101m, 1079s, 1054s, 1028vs, 1003s, 946m, 938m, 862m, 795m, 753m, 721m, 706m, 684m, 653w, 607m, 577m, 529m, 474m, 448w (KBr).

SCHEME 1

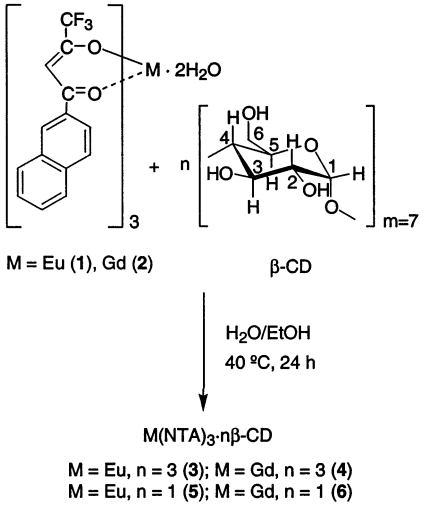

NTA·β-CD (7). A solution of 1-(2-naphthoyl)-3,3,3-trifluoroacetone (0.02 g, 0.076 mmol) in ethanol (2 mL) was added dropwise to a solution of β-CD (0.1 g, 0.076 mmol) in water (5 mL), and the mixture was kept at 40 °C for 24 h. The mixture was centrifuged, the supernatant was decanted, and the pale yellow powder was washed with water and dried in air at room temperature. Yield: 0.09 g, 75%. Anal. Calcd. for (C$_{14}$H$_9$F$_3$O$_2$)·(C$_{42}$H$_{70}$O$_{35}$)·10H$_2$O (1581.4): C, 42.53; H, 6.31. Found: C, 42.27; H, 6.10. Selected ν_{max}/cm^{-1} 2928vs, 1663sh, 1626vs, 1603sh, 1414s, 1387s, 1368s, 1334s, 1298s, 1279s, 1189sh, 1156s, 1080s, 1029s, 1003sh, 945s, 937s, 861m, 802m, 761s, 704s, 607m, 577s, 529s, 476s (KBr).

Results and Discussion

Preparation of Inclusion Compounds. β-Cyclodextrin inclusion compounds containing the lanthanide complexes Eu(NTA)$_3$·2H$_2$O (**1**) and Gd(NTA)$_3$·2H$_2$O (**2**) were prepared by treating a saturated aqueous solution of β-CD with a solution of the complex in ethanol (Scheme 1). The molar ratio of host to guest in the reaction was either 3:1 or 1:1, leading to products designated as M(NTA)$_3$·3β-CD [M = Eu (**3**), Gd (**4**)] and M(NTA)$_3$·β-CD [M = Eu (**5**), Gd (**6**)]. The compounds precipitated from the reaction mixtures as microcrystalline yellow powders and were isolated by centrifugation, rinsed with water, and air-dried at ambient temperature. Elemental analysis indicated host-to-guest ratios close to 3:1 for **3** and **4**, and 1:1 for **5**. The three compounds **3**−**5** were obtained in good yields on the basis of the formation of 3:1 or 1:1 stoichiometric inclusion compounds. By contrast, compound **6** could not be obtained in analytically pure form for a 1:1 complex. The yield was low and elemental analysis indicated an overall host-to-guest ratio of about 2.1:1.

The two europium-containing products **3** and **5** gave rise to substantially different powder XRD patterns (Figure 1). By comparison with the patterns of pristine β-CD hydrate and the "free" complex Eu(NTA)$_3$·2H$_2$O (**1**), it is evident that neither **3** nor **5** contain measurable amounts of phases corresponding to the pure components β-CD and **1**. This is an initial indication

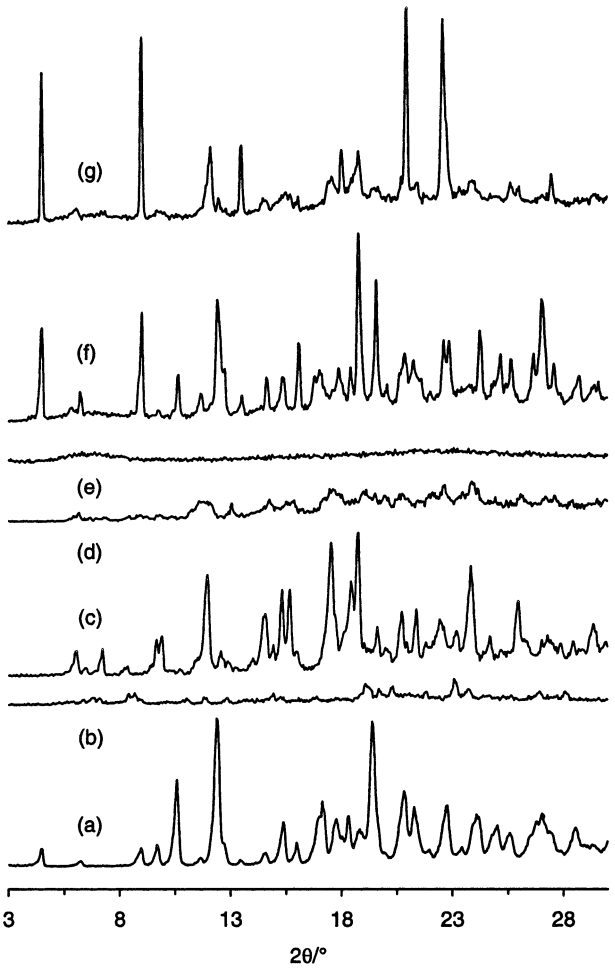

Figure 1. Powder XRD of (a) pristine β-CD hydrate, (b) precursor $Eu(NTA)_3 \cdot 2H_2O$ (**1**), (c) inclusion compound $Eu(NTA)_3 \cdot 3\beta$-CD (**3**), (d) inclusion compound $Eu(NTA)_3 \cdot \beta$-CD (**5**), (e) precursor $Gd(NTA)_3 \cdot 2H_2O$ (**2**), (f) inclusion compound $Gd(NTA)_3 \cdot 3\beta$-CD (**4**), and (g) inclusion compound $Gd(NTA)_3 \cdot \beta$-CD (**6**).

for the formation of true inclusion compounds.[11] It is clear that the compound $Eu(NTA)_3 \cdot 3\beta$-CD (**3**) is the more highly crystalline of the two samples. Also shown in Figure 1 are the powder XRD patterns for the two gadolinium-containing products **4** and **6**. The pattern of **4** matches quite well with that of pure β-CD hydrate, although there are some substantial changes in the intensities of some peaks with some slight changes in the 2θ values. These differences are most pronounced for the low angle peaks up to about 20° 2θ, in particular, the intense peaks at 19.6 and 9.8 Å. These two peaks are also present in the pattern of **6**, suggesting that **6** may in fact be a mixture of phases (1:1, 2:1, and 3:1) giving rise to a bulk analysis of 2.1:1. The precursor gadolinium complex **2** is X-ray amorphous and therefore its presence in the adducts **4** and **6** cannot be ruled out on the basis of these results.

Figure 2 shows the results of thermogravimetric analysis of $Eu(NTA)_3 \cdot 3\beta$-CD (**3**), the complex $Eu(NTA)_3 \cdot 2H_2O$ (**1**), pristine β-CD hydrate, and a physical mixture of β-CD and **1** in a 3:1 molar ratio. TGA of β-CD shows loss of hydrated water up to 75 °C (15.2%, 11−12 water molecules per β-CD molecule). There is no further change until about 235 °C when the compound starts to melt and decompose, characterized by a peak in the differential thermogravimetric (DTG) profile at 294 °C. At 500 °C, 100% mass loss is complete. TGA of the europium chelate **1** shows 1.7% mass loss up to 75 °C which tallies well with the removal of 1 coordinated water molecule. The

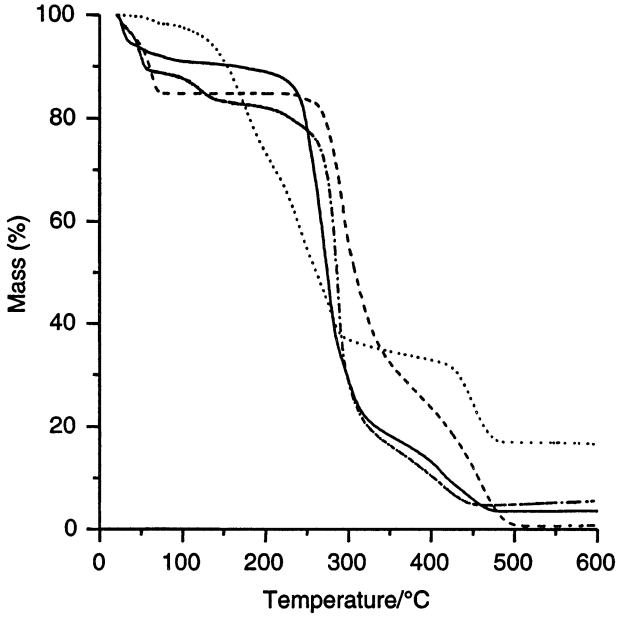

Figure 2. TGA of the inclusion compound $Eu(NTA)_3 \cdot 3\beta$-CD (**3**) (—), precursor $Eu(NTA)_3 \cdot 2H_2O$ (**1**) (•••), pristine β-CD hydrate (− − −), and a physical mixture of β-CD and **1** in a 3:1 molar ratio (− - − -).

compound then decomposes in two steps up to 500 °C, leaving a residual mass of 16.9%. In the case of the physical mixture, each component behaves independently. Steps are visible in the TG profile corresponding to the stages where dehydration of β-CD takes place, the complex **1** decomposes, and β-CD melts and decomposes. The TG behavior of the inclusion compound **3** is very different from that of the physical mixture. There is an initial mass loss of 5.1% up to 35 °C, followed by a more prolonged mass loss of 3.9% up to 100 °C (for comparison, the physical mixture undergoes 12.2% mass loss from room temperature up to 100 °C). There are no steps characteristic of loss of hydrated water from pure β-CD hydrate or decomposition of "free" europium chelate **1**. The results indicate that the europium chelate molecules in **3** are isolated from each other by inclusion complexation with β-CD molecules. Decomposition of **3** is characterized by an abrupt mass loss of 68.2% between 210 and 330 °C (DTG_{max} = 275 °C). Further heating to 500 °C gives a residual mass of 3.5%.

TG analysis was also useful for the recognition of complex formation in the adducts **4**−**6** (Figure 3). The main difference between the thermal behavior of **5** and that of **3** is that decomposition of **5** is extended over a wider temperature range. Otherwise, the observations outlined above for **3** also apply to **5**. Comparable results were obtained for $Gd(NTA)_3 \cdot 2H_2O$ (**2**) and its β-CD adducts.

The KBr IR spectra of compounds **3**−**6** show the typical bands previously reported for bulk KBr spectra of β-CD, indicating no chemical modification of the cyclodextrin host.[12] In addition, several characteristic absorption bands of the guest are observed. The small or nonexistent shifts in the positions of these bands relative to those of the "free" tris(β-diketonate) complexes indicates that the structural integrity of the rare earth chelate complexes **1** and **2** is largely retained upon inclusion complexation with β-CD. It follows that the host−guest interactions are not particularly strong.

Figure 4 shows the ^{13}C CP MAS NMR spectra of $Eu(NTA)_3 \cdot 3\beta$-CD (**3**), $Eu(NTA)_3 \cdot \beta$-CD (**5**), $Eu(NTA)_3 \cdot 2H_2O$ (**1**), and pristine β-CD hydrate. The spectrum of β-CD hydrate is similar to that reported previously and exhibits multiple resonances for

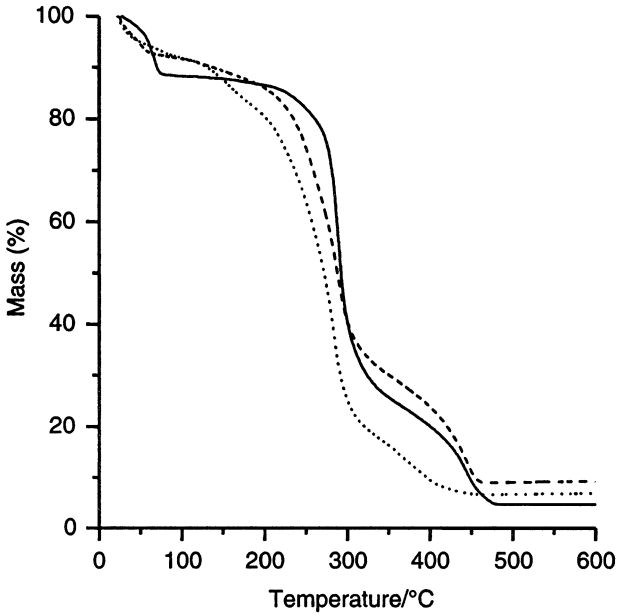

Figure 3. TGA of the inclusion compounds $Gd(NTA)_3 \cdot 3\beta$-CD (**4**) (—), $Eu(NTA)_3 \cdot \beta$-CD (**5**) (•••), and $Gd(NTA)_3 \cdot \beta$-CD (**6**) (– – –).

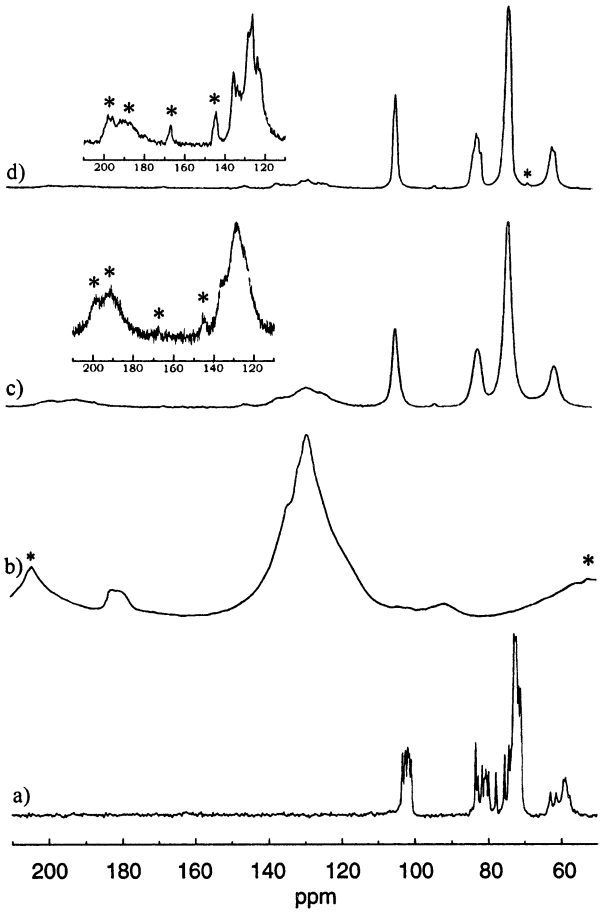

Figure 4. Solid-state ^{13}C CP MAS NMR spectra of (a) pristine β-CD hydrate, (b) precursor $Eu(NTA)_3 \cdot 2H_2O$ (**1**), (c) inclusion compound $Eu(NTA)_3 \cdot \beta$-CD (**5**), and (d) inclusion compound $Eu(NTA)_3 \cdot 3\beta$-CD (**3**). Spinning sidebands are denoted by *.

each type of carbon atom.[13] This has been mainly correlated with different torsion angles about the (1→4) linkages for C-1 and C-4,[13a,b] and with torsion angles describing the orientation of the hydroxyl groups (see Scheme 1 for numbering).[13c] The different carbon resonances are assigned to C-1 (101−104 ppm),

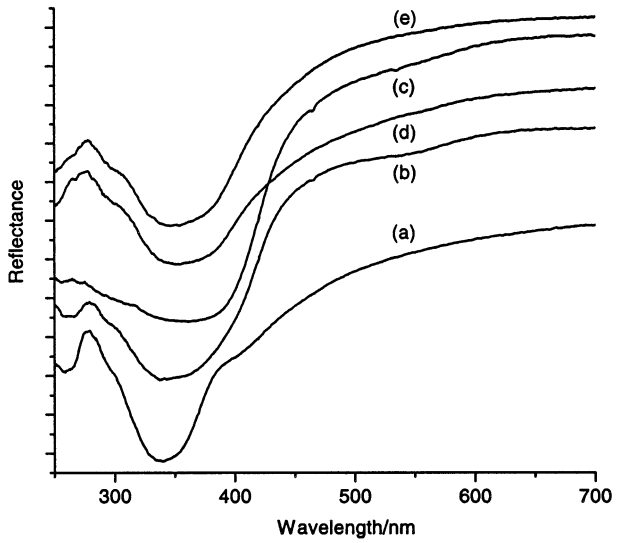

Figure 5. Room-temperature diffuse reflectance spectra of (a) $Eu(NTA)_3 \cdot 2H_2O$ (**1**), (b) $Eu(NTA)_3 \cdot \beta$-CD (**5**), (c) $Eu(NTA)_3 \cdot 3\beta$-CD (**3**), (d) $Gd(NTA)_3 \cdot \beta$-CD (**6**), and (e) $Gd(NTA)_3 \cdot 3\beta$-CD (**4**).

C-4 (78−84 ppm), C-2,3,5 (71−76 ppm), and C-6 (57−65 ppm). By contrast, the corresponding β-CD carbons for the inclusion compounds **3** and **5** are observed as single broad peaks at 103.7, 81.3, 72.9, and 60.5 ppm, respectively. Similar results are obtained when β-CD encapsulates organometallic complexes containing cyclopentadienyl and indenyl groups.[14] A possible interpretation is that the β-CD molecules adopt a more symmetrical conformation in the complex, with each glucose unit in a similar environment, as a direct consequence of the inclusion of aromatic groups in the host cavities.[15] Inclusion compounds of naphthalene or naphthalene derivatives in CDs generally exhibit host−guest stoichiometries of either 1:1 and/or 2:1 in solution and in the solid-state.[16]

The ^{13}C CP MAS NMR spectra of the inclusion compounds **3** and **5** each contain resonances for the carbon atoms of the guest molecules. Both spectra contain a single peak at 93 ppm due to −CO*C*HCO−. In the case of $Eu(NTA)_3 \cdot \beta$-CD (**5**), the naphthalene ring carbon atoms give rise to a broad peak centered at 129 ppm (with a shoulder at 134 ppm). By contrast, the corresponding signals in the spectrum of $Eu(NTA)_3 \cdot 3\beta$-CD (**3**) are much better resolved and several sharp peaks are observed for different carbon atoms. The spectra indicate that the naphthalene groups in **5** exist in a broader range of chemical environments than those in **3**. This is consistent with a model for **3** in which each naphthoyl group in a tris(chelate) complex is encapsulated within one β-CD molecule, thereby giving an inclusion compound with a host−guest stoichiometry of 3:1. In the case of **5**, the existence of 1:1 stoichiometric inclusion complexes would mean that some naphthalene groups are encapsulated within β-CD cavities while others are not. As a final point, it is worth noting that different geometrical isomers are possible for the 8-coordinate complex $Eu(NTA)_3 \cdot 2H_2O$ (**1**),[17] and it is not inconceivable that these would interact differently with β-CD. However, the combination of different ligands (H_2O and NTA) and unsymmetrical ligands (NTA) means that there are many possibilities for geometrical isomers. As a result the spectral identification of these isomers is not possible.

Luminescence Behavior. The room-temperature diffuse reflectance spectra of the complex $Eu(NTA)_3 \cdot 2H_2O$ (**1**) and the inclusion compounds $Eu(NTA)_3 \cdot 3\beta$-CD (**3**), $Eu(NTA)_3 \cdot \beta$-CD (**5**), $Gd(NTA)_3 \cdot 3\beta$-CD (**4**), and $Gd(NTA)_3 \cdot \beta$-CD (**6**) are shown in Figure 5. The spectra are very similar, consisting of a large

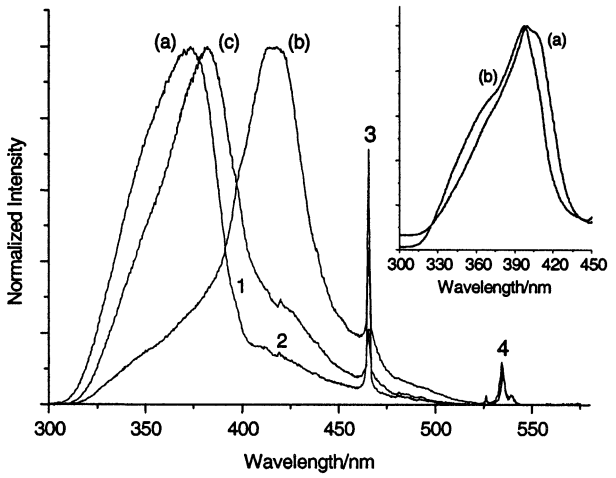

Figure 6. Room-temperature excitation spectra of (a) $Eu(NTA)_3 \cdot 2H_2O$ (**1**), (b) $Eu(NTA)_3 \cdot 3\beta$-CD (**3**), and (c) $Eu(NTA)_3 \cdot \beta$-CD (**5**). The spectra are monitored at the strongest $^5D_0 \rightarrow {}^7F_2$ emission component. (1), (2), (3): $^7F_0 \rightarrow {}^5L_6, {}^5D_3, {}^5D_2$. (4): $^7F_{0,1} \rightarrow {}^5D_1$. The inset shows the excitation spectra of (a) $Gd(NTA)_3 \cdot 3\beta$-CD (**4**) and (b) $Gd(NTA)_3 \cdot \beta$-CD (**6**) (detection wavelengths of 548 nm). These excitation spectra are similar to the corresponding spectra of europium inclusion compounds monitored at the ligand emission (see Figure 9).

broad absorption band in the UV region at approximately 300−400 nm. The maximum of this band is at higher wavelengths in the inclusion compounds, relative to the precursor complexes, and shifts toward lower energies as the molar ratio of host to guest increases from 1:1 to 3:1.

Figure 6 shows the room-temperature excitation spectra of the complex $Eu(NTA)_3 \cdot 2H_2O$ (**1**) and the inclusion compounds $Eu(NTA)_3 \cdot 3\beta$-CD (**3**) and $Eu(NTA)_3 \cdot \beta$-CD (**5**). The spectra present a large broad band between 320 and 450 nm and a series of sharp lines characteristic of the Eu^{3+}energy level structure, assigned to transitions between the $^7F_{0,1}$ and the $^5L_6, {}^5D_{3,2,1}$ levels. Comparing the excitation spectrum of **1** with those of the inclusion compounds, a significant displacement for the lower energy region of the maximum of the broad band is detected. Furthermore, this shift is more pronounced as the molar ratio of host to guest increases from 1:1 to 3:1, in accordance with the diffuse reflectance data. This may be induced by the encapsulation of each naphthoyl group in a tris(chelate) complex within one β-CD molecule, thereby giving an inclusion compound with a host-to-guest stoichiometry of 3:1, as mentioned above.

The large broad band may be related to excited states of the ligands or to ligand-to-metal charge-transfer (LMCT) transitions resulting from the interaction between the ion and the ligands first coordination shell.[8,18−20] To verify if the nature of this band is related with LMCT states, the excitation spectra of the Gd^{3+}-based compounds were recorded. The Gd^{3+} luminescence spectra are a useful tool because the energetic difference between the first excited state and the fundamental levels is too high to allow the detection of charge transfer states in the ultraviolet/visible range. Since a similar broad band is discerned in the excitation spectra of the gadolinium β-CD adducts (inset of Figure 6), the possibility of LMCT transitions is completely ruled out and, therefore, the broad band is ascribed to transitions populating singlet and triplet excited states localized in the naphthoyl ligands. A definitive assignment of the emitting excited states lies beyond the scope of this work since it requires molecular orbital calculations.[8,21]

The displacement for the lower energy region of the maximum of the broad excitation band mentioned above for

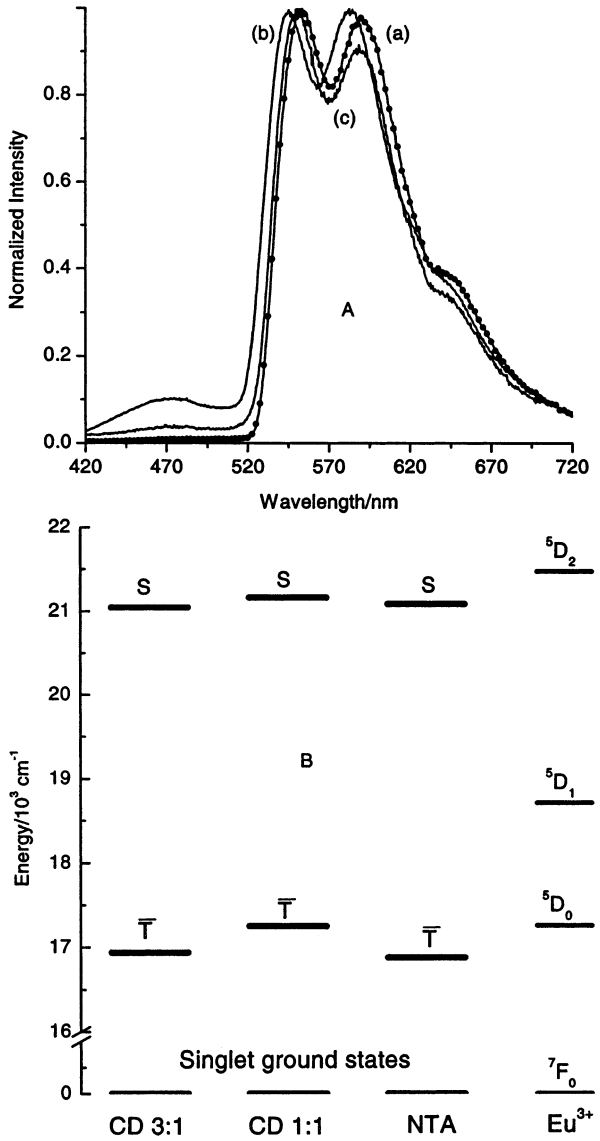

Figure 7. A: Emission spectra (14 K) of (a) precursor $Gd(NTA)_3 \cdot 2H_2O$ (**2**) (solid line with dots), (b) inclusion compound $Gd(NTA)_3 \cdot 3\beta$-CD (**4**), and (c) inclusion compound $Gd(NTA)_3 \cdot \beta$-CD (**6**). The excitation wavelengths are 400 and 398 nm, for the precursor complex and the inclusion compounds, respectively. B: Schematic illustration of the energy level diagram of ligand and Eu^{3+} excited states in the precursor complex and in the Eu^{3+}-based β-CD adducts.

the Eu^{3+} compounds indicates that the interaction of the precursor salt with the β-CD host structure, with the concomitant formation of inclusion complexes, changes the energy of the ligand excited states, relative to the Eu^{3+} ones. These energy changes were quantitatively estimated by recording the phosphorescence spectra and measuring the decay times of the ligand excited states for the compounds $Gd(NTA)_3 \cdot 2H_2O$ (**2**), $Gd(NTA)_3 \cdot 3\beta$-CD (**4**), and $Gd(NTA)_3 \cdot \beta$-CD (**6**). Since the spectral resolution is higher at lower temperatures, the phosphorescence was recorded at 14 K (Figure 7). The spectra are actually composed of three distinct bands, corresponding to the emission from the lowest three triplet states, each localized in a NTA ligand molecule. The lifetime was measured at 300 K (excitation wavelength of 380 nm) and detected at the strongest emission component, at about 583 and 590 nm for the 1:1 and 3:1 adducts, respectively. The values found, 1.804 ± 0.068 ms for **4** and 1.422 ± 0.076 ms for **6**, are consistent with emission from a state with strong triplet character.[21] The weak band seen in

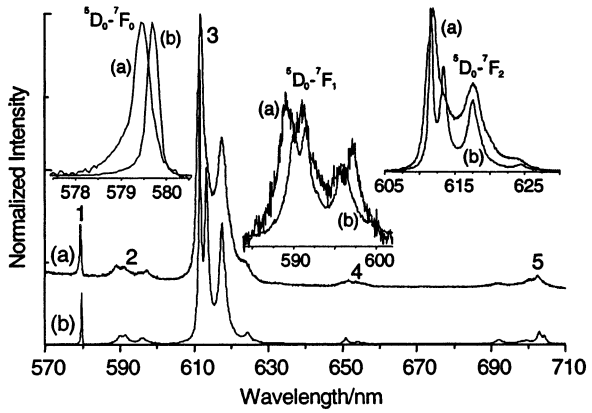

Figure 8. Room-temperature emission spectra of inclusion compounds (a) Eu(NTA)$_3$·3β-CD (**3**) and (b) Eu(NTA)$_3$·β-CD (**5**). (1), (2), (3), (4), (5): $^5D_0 \rightarrow {}^5F_{0-4}$. The excitation wavelengths are 420 and 382 nm, respectively. The regions of the $^5D_0 \rightarrow {}^5F_{0,1,2}$ transitions are displayed in detail.

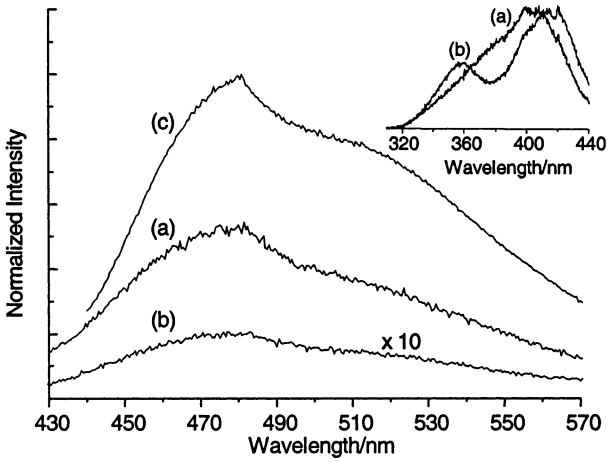

Figure 9. Detail of the room-temperature emission spectra (430−570 nm) of (a) Eu(NTA)$_3$·3β-CD (**3**) and (b) Eu(NTA)$_3$·β-CD (**5**). The curve (c) is the emission spectrum of the NTA ligand alone incorporated into β-CD (**7**) (excitation wavelength of 425 nm). The inset shows the room-temperature excitation spectra of the two inclusion compounds monitored at the large broad band.

Figure 7 at ca. 470 nm (much more evident in the inclusion compounds) could be associated with fluorescence from excited singlet states of the ligands. The lifetime of this emission could not be performed since it lies out of the range scale of the experimental setup used (smaller than 10^{-4} s). This is in agreement with emission from a state with singlet nature. Part B of Figure 7 shows the energy level diagram of ligand and Eu^{3+} excited states in the precursor salt and in the two inclusion compounds. A deconvolution Gaussian-type fitting procedure was applied both to the singlet and triplet ligand states. For the latter states an average value for the three NTA ligands is given.

The room-temperature emission spectra of the inclusion compounds Eu(NTA)$_3$·3β-CD (**3**) and Eu(NTA)$_3$·β-CD (**5**) are shown in Figure 8. The spectrum of the former compound is very similar to the one characteristic of the precursor complex.[9] The spectra present the $^5D_0 \rightarrow {}^7F_J$ ($J = 0-4$) sharp lines characteristic of the Eu^{3+} energy level structure and a large, structured broad band at lower wavelengths (maximum around 480 nm), which is particularly evident for **3** (Figure 9). Excitation spectra monitored around the maximum of the broad emission (475−480 nm) permit us to ascribe unequivocally this band to the luminescence of the ligands, as the inset of Figure 9 illustrates. In fact, these excitation spectra are very similar to the ones obtained for the gadolinium-based inclusion compounds (inset of Figure 6). Therefore, bearing in mind the absence of any Gd^{3+} excited state in that energy range, the structured band profile must be associated with excited states of the ligands, indicating that the inclusion of the complex into the β-CD cavity induces an inefficient energy transfer pathway between the ligands and the metal ion. Moreover, as the integrated intensity of the broad band relative to the Eu^{3+} emission increases as the molar ratio of host-to-guest increases from 1:1 to 3:1 (Figure 9), the energy transfer pathway becomes more inefficient when each naphthoyl group in a tris(chelate) complex is encapsulated within one β-CD molecule. The broad ligand-related emission and the corresponding inefficient energy transfer step are not observed in the analogous 1:1 inclusion compound between Eu(NTA)$_3$·2H$_2$O and γ-CD,[22] probably due to a better accommodation of the luminescent complex within the cyclodextrin cavity.

The room-temperature lifetime of the broad ligand-related emission lies out of the range scale of our experimental setup (smaller than 10^{-4} s), as the weak band seen in the emission spectra of the gadolinium β-CD adducts (Figure 7). In addition, as the energy range and the profile of these two bands are very similar, this emission could originate in the singlet excited state of the ligands. This means that internal conversion and intersystem crossing between the singlet level and the lowest triplet state of the ligands seems to be inoperative, in particular for the adduct Eu(NTA)$_3$·3β-CD (**3**) since the singlet emission is substantially raised relative to that of Eu(NTA)$_3$·β-CD (**5**). The emission spectrum of the NTA ligand alone incorporated into β-CD (**7**) presents a large broad band, the energy range and profile of which are exactly the same as the bands characteristic of the spectra of the Eu^{3+}−β-CD inclusion compounds (Figure 9). The measured lifetime also lies out of the range scale of our experimental setup (smaller than 10^{-4} s). This provides additional evidence supporting the previous assignment of the broad emission to phosphorescence from the singlet excited state of the naphthoyl ligands.

When we compare the emission spectra of Eu(NTA)$_3$·3β-CD (**3**) and Eu(NTA)$_3$·β-CD (**5**) for the $^5D_0 \rightarrow {}^7F_{0-4}$ transitions (Figure 8), changes are observed in the energy, maximum splitting and profile of these bands (essentially in the $^5D_0 \rightarrow {}^7F_{0,1,2}$ ones). The energy of the $^5D_0 \rightarrow {}^7F_0$ line and its full width at half-maximum increase as the molar ratio of host to guest increases (from 17250.23 ± 0.04 to 17257.69 ± 0.14 cm^{-1} and from 7.94 ± 0.08 to 13.33 ± 0.28 cm^{-1}, respectively, on going from 1:1 to 3:1). Moreover, the maximum splitting of the $^7F_1$ manifold, $\Delta E(^7F_1)$, which is associated with the overall electrostatic energy of the Eu^{3+} local environments,[23] also increases (from 166 to 230 cm^{-1}) as the molar ratio of host-to-guest increases. Furthermore, the local-field splitting of the $^5D_0 \rightarrow {}^7F_2$ transition in, at least, five Stark components is much more evident in the inclusion compound **5**. The number of Stark components detected for the $^5D_0 \rightarrow {}^7F_{1-4}$ transitions in both spectra indicate that the Eu^{3+} ions occupy a very low site symmetry without inversion center, according to the high intensity of the $^5D_0 \rightarrow {}^7F_2$ transition.

The room temperature $^5D_0$ decay curves (detected at the strongest $^5F_2$ Stark level) of the inclusion compounds Eu(NTA)$_3$·3β-CD (**3**) and Eu(NTA)$_3$·β-CD (**5**) are shown in Figure 10. For values larger than 0.28 and 0.88 ms, for **3** and **5,** respectively, the curves are well fitted by a single-exponential function with corresponding $^5D_0$ lifetimes around 0.325 ± 0.003 and 0.221 ± 0.002 ms, respectively. Both values are smaller than the one characteristic of the complex, 0.356 ± 0.003 ms.[9]

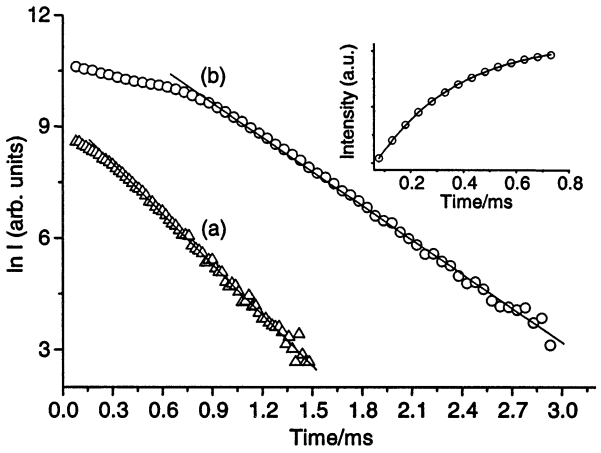

Figure 10. Room-temperature $^5D_0$ decay curves for the inclusion compounds (a) Eu(NTA)$_3$·3β-CD (**3**) and (b) Eu(NTA)$_3$·β-CD (**5**). The excitation wavelength is 420 and 380 nm, respectively. The straight lines represent the best fits ($r^2 = 0.999$) to the data considering a single-exponential behavior. The inset shows the "grow-in" component of the luminescent emission profile of Eu(NTA)$_3$·β-CD (**5**). The solid line is a fit to the data ($r^2 = 0.999$) considering an exponential growth function.

For shorter times, the decay profiles unequivocally exhibit nonexponential behavior, particularly evident for **5** (Figure 10), indicating therefore that the decay curves have other contributions for shorter times. Indeed, when the single-exponential component is subtracted from the measured intensity in that time range, we found a "grow-in" behavior (or rise-time), particularly evident for **5** (inset of Figure 10). This indicates that the luminescence decay curves might have a contribution from a ligand-to-metal ion energy transfer pathway, providing additional evidence for the presence of an inefficient energy transfer step as the naphthoyl moiety is incorporated into the β-CD cavity, either as a result of its slow forward rate or of a significant back transfer process.[24] Since the singlet emission relative to the Eu^{3+} one is substantially raised as the molar ratio of host to guest increases from 1:1 to 3:1 (with the corresponding decrease in the efficiency of the singlet-lowest triplet internal conversion and intersystem crossing), the contribution of that energy transfer pathway for the $^5D_0$ decay profile decreases as the host−guest stoichiometry increases.

All these aspects seem to indicate that encapsulation of the complex Eu(NTA)$_3$·2H$_2$O into the host β-CD cage modifies essentially the second Eu^{3+} coordination shell, particularly the energy and the lifetime of the triplet state of the naphthalene groups. In the following, this conclusion will be quantitatively stressed by calculating the experimental intensity parameters Ω_2 and Ω_4.

The emission intensity I, taken as the surface S of the emission curves, for the $^5D_0 \rightarrow {}^7F_{1,2,4}$ transitions, is expressed by

$$I_{i\rightarrow j} = \hbar\omega_{i\rightarrow j} A_{i\rightarrow j} N_i \equiv S_{i\rightarrow j} \qquad (1)$$

where i and j represent the initial ($^5D_0$) and final ($^7F_{0-4}$) levels, respectively, $\hbar\omega_{i\rightarrow j}$ is the transition energy, $A_{i\rightarrow j}$ the corresponding Einstein's coefficient of spontaneous emission, and N_i the population of the emitting level ($^5D_0$).[21,25] Usually the experimental intensity parameters are obtained from absorption data. However, in the case of Eu^{3+} the pure magnetic dipolar character displayed by the $^5D_0 \rightarrow {}^7F_1$ transition allows the determination of the intensity parameters from emission spectra. This transition does not depend on the local ligand field seen by Eu^{3+} ions and thus may be used as a reference for the whole spectrum, $A(^5D_0 \rightarrow {}^7F_1) \approx 50\ s^{-1}$.[8,21,25] In addition, the electric dipolar $^5D_0 \rightarrow {}^7F_{2,4,6}$ transitions depend only on the $U^{(2)}$, $U^{(4)}$, and $U^{(6)}$ reduced matrix elements, respectively, which allows the evaluation of the experimental intensity $\Omega_{2,4,6}$ parameters directly from emission data. On the basis of the luminescence spectra for the inclusion compounds Eu(NTA)$_3$·3β-CD (**3**) and Eu(NTA)$_3$·β-CD (**5**) (Figure 8), the experimental intensity parameters Ω_2 and Ω_4 were determined using the $^5D_0 \rightarrow {}^7F_2$ and $^5D_0 \rightarrow {}^7F_4$ transitions, respectively. The $A_{i\rightarrow j}$ Einstein coefficient is given by[21]

$$A_{i\rightarrow j} = \frac{4e^2\omega^3}{3\hbar c^3}\frac{1}{2J+1}\chi\sum_{\lambda}\Omega_\lambda\langle {}^7F_J\|U^{(\lambda)}\|{}^5D_0\rangle^2 \qquad (2)$$

where ω is the frequency of the transition and $\chi = n_0(n_0^2 + 2)^2/9$, a Lorentz local field correction for the index of refraction n_0 of the medium. The reduced matrix elements in eq 2 were taken from Carnall et al.[26] and an average index of refraction equal to 1.5 was used.[6,8,25] The Ω_6 intensity parameter was not determined because the $^5D_0 \rightarrow {}^7F_6$ transition could not be experimentally detected for **3** and **5**. This stresses therefore that Ω_6 is not important here. The obtained values for Ω_2 and Ω_4 (in units of 10^{-20} cm^2) are 27.7 and 4.99 for Eu(NTA)$_3$·3β-CD (**3**), 30.5 and 4.74 for Eu(NTA)$_3$·β-CD (**5**).

The interpretation of the physical meaning of the phenomenological Judd-Ofelt intensity parameters still remains a controversial matter for discussion. There is, in fact, a long story in the literature trying to relate the observed variations with some specific ligand field effects.[27] Ω_2 variations are usually related to the degree of covalency in the lanthanide−first coordination shell interaction.[21,25,27−29] In the sense of the dynamic coupling contribution to the total intensity,[29] the polarization of the ligand field induces stronger lanthanide−ligand bonds and an increase in electric dipolar transitions for noncentrosymmetric ligand fields. On the other hand, $\Omega_{4,6}$ parameters have been related together to bulk properties of the lanthanide-based hosts (viscosity, for instance).[21,25,27−29] There is no theoretical prediction for this sensibility to macroscopic properties, but empirical variations seem to suggest some kind of relationship. The relatively high value results for Ω_2 indicate a highly polarizable Eu^{3+} local environment in these compounds.[6,8,21,25] Comparison with the values found for the precursor complex (27.8 and 3.74 × 10^{-20} cm^2, for Ω_2 and Ω_4, respectively[9]), we note very similar values for the former intensity parameter and an increase of the value of Ω_4 as the complex is incorporated into the β-CD host. This seems to point out that there is no appreciable variation of the polarizability of the first coordination shell for the inclusion compounds and that the steric effects are more significant in the supramolecular inclusion compounds, as expected by the encapsulation of one naphthoyl group within one β-CD molecule. This is also observed for other similar Eu^{3+}-based β−CD inclusion compounds.[6]

Conclusions

Inclusion compounds with different host-to-guest ratios have successfully been prepared between β-cyclodextrin and rare earth tris(β-diketonates). Characterization in the solid-state by powder XRD, TGA, FTIR, and ^{13}C CP MAS NMR spectroscopy supports the formation of true inclusion compounds in which the naphthoyl moieties of the guest species are encapsulated within the β-CD cavities. The photoluminescence results indicate that this encapsulation seems to modify essentially the second Eu^{3+} coordination shell, particularly the energy and the

lifetime of the lowest triplet state of the naphthalene groups. In fact, comparing the experimental intensity parameters Ω_2 and Ω_4 for the complex and for the two inclusion compounds, we conclude that there is no appreciable variation of the polarizability of the first coordination shell and that the steric effects are more significant in the supramolecular inclusion compounds, as expected by the encapsulation of the naphthoyl moieties into the β-CD cavity. Furthermore, it is concluded that encapsulation induces emission from the singlet excited state of the ligands with the corresponding presence of an inefficient ligand-to-metal energy transfer step, clearly detected in the $^5D_0$ decay profiles, a situation which does not occur in analogous adducts involving γ-CD which have a larger inclusion cavity.

Acknowledgment. We are grateful to PRAXIS XXI (BD/18404/98) for partial funding. We also thank J. F. S. Menezes for the synthesis of the $M(NTA)_3 \cdot 2H_2O$ complexes and Marta Lopes for assistance in the NMR experiments.

References and Notes

(1) (a) Szejtli, J. *Chem. Rev.* **1998**, *98*, 1743. (b) Szejtli, J. In *Comprehensive Supramolecular Chemistry*; Szejtli, J., Osa, T., Eds.; Pergamon: Oxford, 1996; Vol. 3, Chapter 5. (c) Saenger, W. *Angew. Chem., Int. Ed. Engl.* **1980**, *19*, 344.

(2) Harata, K. In *Comprehensive Supramolecular Chemistry*; Szejtli, J., Osa, T., Eds.; Pergamon: Oxford, 1996; Vol. 3, Chapter 9.

(3) Fenyvesi, E.; Szente, L.; Russel, N. R.; McNamara, M. In *Comprehensive Supramolecular Chemistry*; Szejtli, J., Osa, T., Eds.; Pergamon: Oxford, 1996; Vol. 3, Chapter 10.

(4) Eaton, D. F.; Anderson, A. G.; Tam, W.; Wang, Y. *J. Am. Chem. Soc.* **1987**, *109*, 1886.

(5) (a) Shimada, M.; Harada, A.; Takahashi, S. *J. Chem. Soc., Chem. Commun.* **1991**, 263. (b) Patel, P. P.; Welker, M. E. *J. Organomet. Chem.* **1997**, *547*, 103.

(6) Brito, H. F.; Carvalho, C. A. A.; Malta, O. L.; Passos, J. J.; Menezes, J. F. S.; Sinisterra, R. D. *Spectrochim. Acta* **1999**, *55*, 2403.

(7) Archer, R. D.; Chen, H.; Thompson, L. C. *Inorg. Chem.* **1998**, *37*, 2089, and references therein.

(8) de Sá, G. F.; Malta, O. L.; De Mello Donegá, C.; Simas, A. M.; Longo, R. L.; Santa-Cruz, P. A.; Silva, E. F., Jr. *Coord. Chem. Rev.* **2000**, *196*, 165.

(9) Carlos, L. D.; De Mello Donegá, C.; Albuquerque, R. Q.; Alves, S., Jr.; Menezes, Y. F. S.; Malta, O. L. *Mol. Phys.*, in press.

(10) Charles, R. G.; Perrotto, A. *J. Inorg. Nucl. Chem.* **1964**, *26*, 373.

(11) Saenger, W. *Angew. Chem., Int. Ed. Engl.* **1980**, *19*, 344.

(12) Sabapathy, R. C.; Bhattacharyya, S.; Cleland, W. E.; Hussey, C. L. *Langmuir* **1998**, *14*, 3797, and references therein.

(13) (a) Gidley, M. J.; Bociek, S. M. *J. Am. Chem. Soc.* **1988**, *110*, 3820. (b) Heyes, S. J.; Clayden, N. J.; Dobson, C. M. *Carbohydr. Res.* **1992**, *233*, 1. (c) Veregin, R. P.; Fyfe, C. A.; Marcessault, R. H.; Tayler, M. G. *Carbohydr. Res.* **1987**, *160*, 41.

(14) (a) Braga, S. S.; Gonçalves, I. S.; Lopes, A. D.; Pillinger, M.; Rocha, J.; Romão, C. C.; Teixeira-Dias, J. J. C. *J. Chem. Soc., Dalton Trans.* **2000**, 2964. (b) Braga, S. S.; Gonçalves, I. S.; Pillinger, M.; Ribeiro-Claro, P.; Teixeira-Dias, J. J. C. *J. Organomet. Chem.* **2001**, *632*, 11. (c) Lima, S.; Gonçalves, I. S.; Ribeiro-Claro, P.; Pillinger, M.; Lopes, A. D.; Ferreira, P.; Teixeira-Dias, J. J. C.; Rocha, J.; Romão, C. C. *Organometallics* **2001**, *20*, 2191.

(15) Li, J.; Harada, A.; Kamachi, M. *Bull. Chem. Soc. Jpn.* **1994**, *67*, 2808.

(16) Kokkinou, A.; Yannakopoulou, K.; Mavridis, I. M.; Mentzafos, D. *Carbohydr. Res.* **2001**, *332*, 85, and references therein.

(17) Fortman, J. J.; Sievers, R. E. *Coord. Chem. Rev.* **1971**, *6*, 331.

(18) Sabbatini, N.; Guardigli, M.; Lehn, J.-M. *Coord. Chem. Rev.* **1993**, *123*, 201.

(19) Carlos, L. D.; Sá Ferreira, R. A.; de Zea Bermudez, V.; Molina, C.; Bueno, L. A.; Ribeiro, S. J. L. *Phys. Rev. B* **1999**, *60*, 10042.

(20) De Mello Donegá, C.; Ribeiro, S. J. L.; Gonçalves, R. R.; Blasse, G. *J. Phys. Chem. Solids* **1996**, *57*, 1727.

(21) (a) Malta, O. L.; Couto dos Santos, M. A.; Thompson, L. C.; Ito, N. K. *J. Lumin.* **1996**, *69*, 77. (b) Malta, O. L.; Brito, H. F.; Menezes, J. F. S.; Gonçalves e Silva, F. R.; Alves, S., Jr.; Farias, F. S., Jr.; de Andrade, A. V. M. *J. Lumin.* **1997**, *75*, 255.

(22) Braga, S. S.; Sá Ferreira, R. A.; Gonçalves, I. S.; Ribeiro-Claro, P.; Pillinger, M.; Rocha, J.; Teixeira-Dias, J. J. C.; Carlos L. D. *J. Inclusion Phenom. Macrocyclic Chem.*, in press.

(23) Lochhead, M. J.; Bray, K. L. *Phys. Rev. B* **1995**, *52*, 15763.

(24) Skinner, P. J.; Beeby, A.; Dickins, R. S.; Parker, D.; Aime, S.; Botta, M. *J. Chem. Soc., Perkin Trans.* **2000**, *2*, 1329.

(25) Carlos, L. D.; Messaddeq, Y.; Brito, H. F.; Sá Ferreira, R. A.; de Zea Bermudez, V.; Ribeiro, S. J. L *Adv. Mater.* **2000**, *12*, 594.

(26) Carnall, W. T.; Crosswhite, H.; Crosswhite, H. M. *Energy Structure and Transition Probabilities of the Trivalent Lanthanides in LaF_3*; Argonne National Laboratory Report, unnumbered, 1977.

(27) Reisfeld, R.; Jörgensen, C. K. In *Handbook on the Physics and Chemistry of Rare Earths*; Gschneidner, K. A., Eyring, L., Eds.; North-Holland: Amsterdam, 1987; Vol. 9, Chapter 58, and references therein.

(28) Oomen, E. W. J. L.; van Dongen, A. M. A. *J. Non-Cryst. Solids* **1989**, *111*, 205.

(29) Judd, B. R. *J. Chem. Phys.* **1979**, *70*, 4830.